Electronic Supplementary Material (ESI) for Polymer Chemistry.
This journal is © The Royal Society of Chemistry 2019

Electronic Supplementary Material (ESI) for Polymer Chemistry.
This journal is © The Royal Society of Chemistry 2019

Electronic Supporting Information

Systematically Investigating the Effect of the Aggregation Behaviors in Solution on the Charge Transport Properties of BDOPV-Based Polymers with Conjugation-Break Spacers

Yi Liu,[a] Xin-Yi Wang,[b] Zi-Yuan Wang,[b] Yang Lu [b] Xiu-Fen Cheng,[a] Bo Tang,*[a] Jie-Yu Wang,[b] Jian Pei*[b]

[a]*College of Chemistry, Chemical Engineering and Materials Science, Collaborative Innovation Center of Functionalized Probes for Chemical Imaging in Universities of Shandong, Key Laboratory of Molecular and Nano Probes, Ministry of Education, Shandong Provincial, Key Laboratory of Clean Production of Fine Chemicals, Shandong Normal University, Jinan, 250014*

[b] *Beijing National Laboratory for Molecular Sciences (BNLMS), Key Laboratory of Polymer Chemistry and Physics of Ministry of Education, Center of Soft Matter Science and Engineering, College of Chemistry and Molecular Engineering, Peking University, Beijing 100871, China.*

Email: tangb@sdnu.edu.cn; jianpei@pku.edu.cn

1. General procedures and experimental details

All commercially available chemicals and solvents are of reagent grade unless otherwise indicated. All air and water sensitive reactions were took place in under N_2 atmosphere. Gel permeation chromatography (GPC) (150 °C, 1,2,4-trichlorobenzene) determined molecular weights by Polymer Laboratories PL-GPC220. Absorption spectra were performed on PerkinElmer Lambda 750 UV-*vis* spectrometer. Varied-temperature absorption spectra were performed on Shimadzu UV3600Plus spectrometer. Thermal gravity analyses (TGA) and differential scanning calorimetry (DSC) analyses were performed on by TA Instrument Q600 analyzer and METTLER TOLEDO Instrument DSC822 calorimeter, respectively. Cyclic Voltammetry (CV) was performed on a SP-300 Bio-Logic potentiostat and measurements were recorded in acetonitrile containing 0.1 M *n*-Bu_4NPF_6 as a supporting electrolyte for polymer thin films, glassy carbon electrode as working electrode and platinum wire as counter electrode. All potentials were recorded versus AgCl/Ag (saturated) as reference electrode (scan rate: 50 mV s^{-1}) and the Fc/Fc^+ redox couple was represented as an external standard. GIWAXS was performed at the College of Chemistry and Molecular Engineering, Peking University.

FET Devices Fabrications and Testing. Top-gate bottom-contact (TG/BC) FET device configuration was adopted using n^{++}-Si/SiO_2 (300 nm) substrates. The gold source and drain bottom electrodes (with Ti as the adhesion layer) were patterned on the SiO_2 surface with photolithography. The substrates were subjected to cleaning using ultrasonication in acetone, detergent, deionized water (twice), isopropanol and then dried under vacuum at 80 °C. The polymer solution (3 mg mL^{-1} in *o*-DCB) was spin-coated on the substrates at 1000 rpm for 60 s and 3000 rpm for 3s. The samples were immediately followed by annealing at 180 °C for 10 min. After annealing, a CYTOP solution (CTL809M/CT-solv180 = 3/1) was spin-coated onto the semiconducting layer at 2000 rpm for 60 s and then annealed at 100 °C for 60 min in a glovebox. 45 nm-thickness Al film was deposited under vacuum (4×10^{-4} Pa) via shadow mask method as the gate electrodes. The testing of the FETs were performed on a probe stage using a Keithley 4200 SCS as parameter analyzer under ambient conditions (22 °C, R_H = 50–60%). The carrier mobility, μ, was calculated from the data in the saturated regime according to the equation $I_{SD} = (W/2L)\, C_i\mu(V_G - V_T)^2$, where I_{SD} is the drain current in the saturated regime. W and L are the width and length of the semiconductor channel, respectively. C_i (C_i = 3.7 nF) is the capacitance per unit area of the gate dielectric layer, and V_G and V_T are the gate voltage and threshold voltages.

Solution Doping and Thin Film Fabrication. *N*-DMBI was mixed with the BDOPV-based copolymers to prepare an *o*-DCB solution with a concentration of 3 mg mL^{-1}. The mixture solution was immediately spin-coated on the treated substrate at 1500 rpm for 60 s and then 3000 rpm for 3 s, followed by annealing at 120 °C for 8 h. The film thickness (~8 nm) is determined by AFM. 4-Point conductivity measurements were performed in an N_2 glovebox with Keithley 4200 SCS.

2. Synthetic procedures and characterization

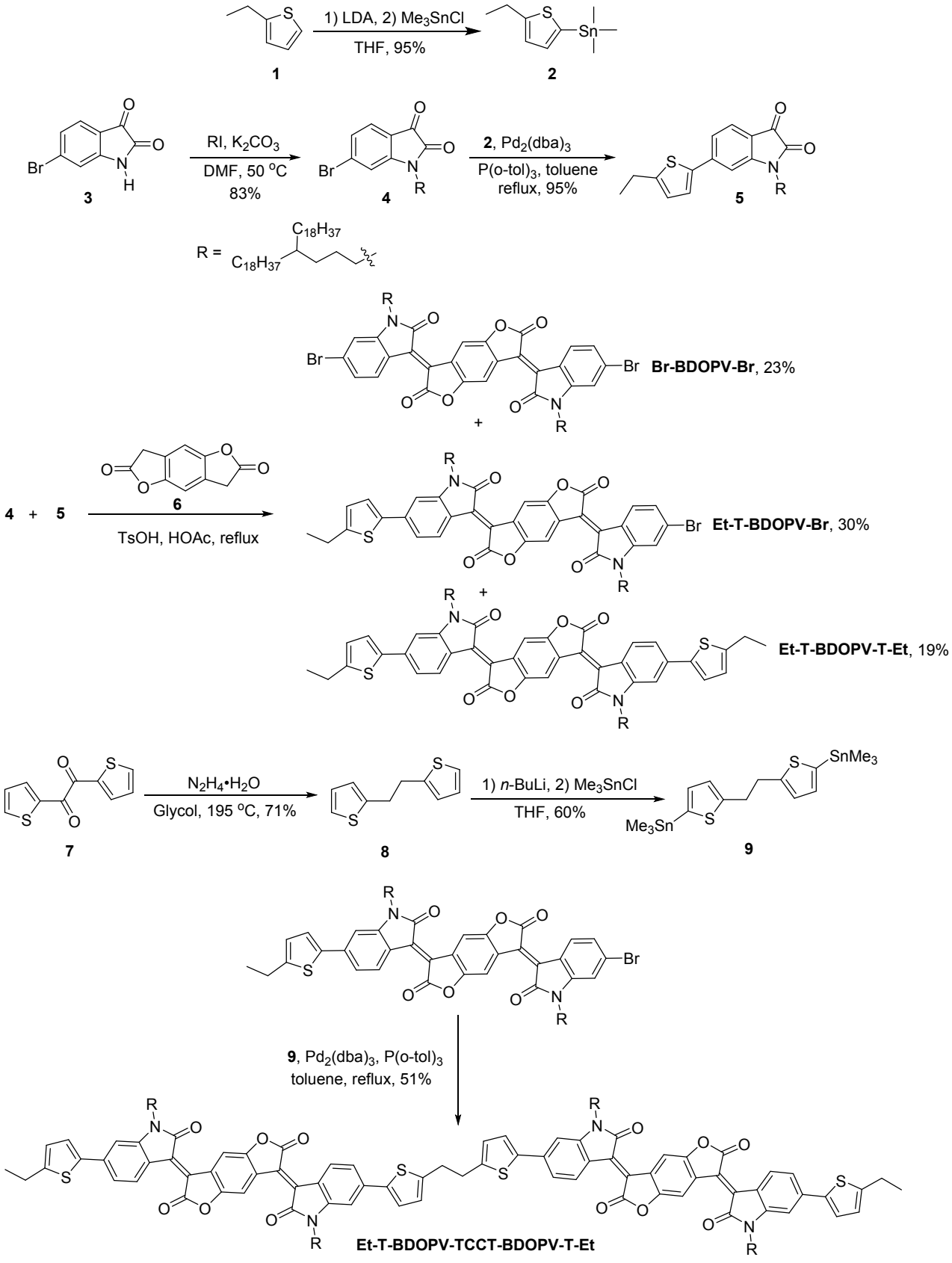

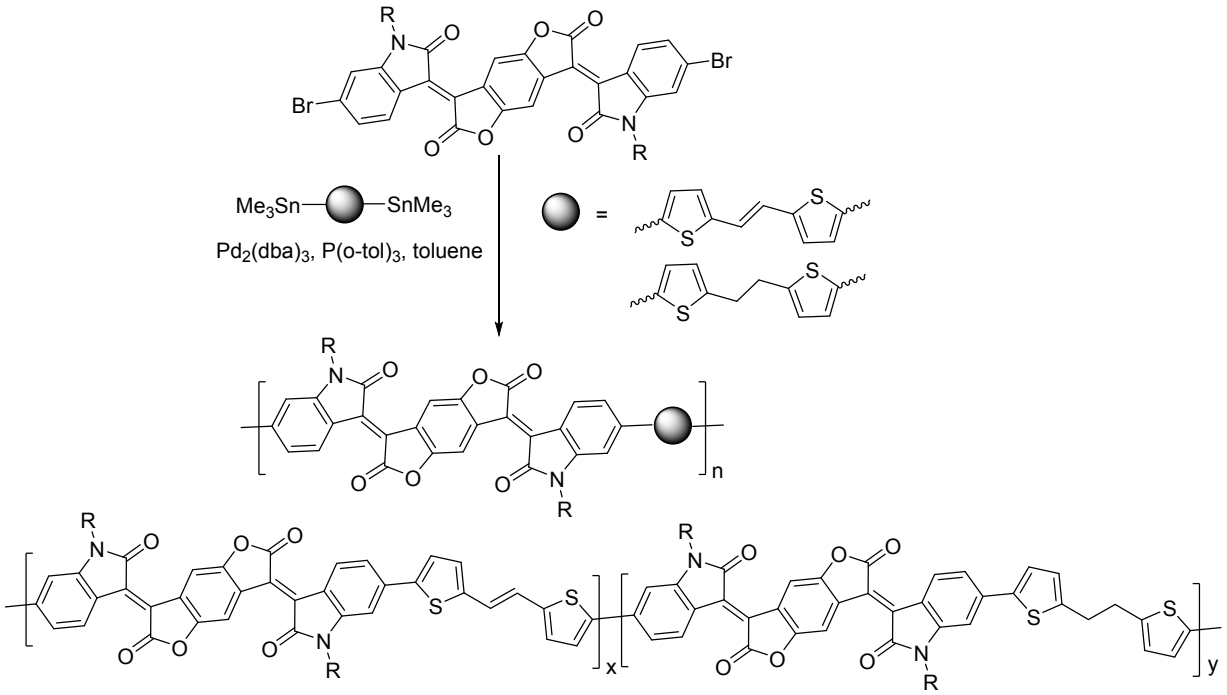

BDOPV-TVT: x = 100%
BDOPV-TVT$_{0.95}$-TCCT$_{0.05}$: x = 95%, y = 5%
BDOPV-TVT$_{0.8}$-TCCT$_{0.2}$: x = 80%, y = 20%
BDOPV-TVT$_{0.5}$-TCCT$_{0.5}$: x = 50%, y = 50%
BDOPVTCCT: y = 100%

Scheme S1. Synthetic route to BDOPV derivatives and five BDOPV-based polymers. Compounds **4**, **6**, **8**, **9**, and **Br-BDOPV-Br** were synthesized according to the literature[1,2,3]

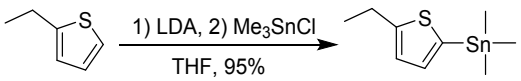

1 **2**

Compound 2: To a solution of *n*-butyllithium (7.4 mL, 2.4 M) in anhydrous tetrahydrofuran (THF) (15 mL), *N*-(1-methylethyl)-2-propanamine (DIPA, 1.80 g, 17.8 mmol) was slowly added under N_2 atmosphere. The mixture was stirred at -78 ^oC for 30 min to prepare lithium diisopropylamide (LDA) for next step. To a solution of 2-ethylthiophene (1 g, 8.9 mmol) in anhydrous THF (15 mL), LDA (1.80 g, 17.8 mmol) was slowly added under N_2 atmosphere. The mixture was stirred at -78 ^oC for 40 min and then added chlorotrimethylstannane (3.55 g, 17.8 mmol) to the mixture for 2 h. The mxiture was quenched with water and then extracted with CH_2Cl_2 (100 mL), and dried over with anhydrous Na_2SO_4. After removal of the solvents under reduced pressure, the residue was directly used for the next step without further purification. Yield: 95%.

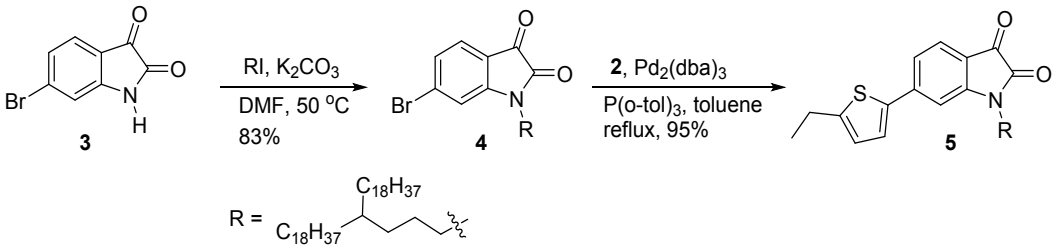

Compound 5: Compound **4** (108.34 mg, 0.137 mmol), **2** (64.35 mg, 0.234 mmol), $Pd_2(dba)_3$ (5.04 mg) and P(*o*-tol)$_3$ (6.710 mg) were added to a 100 mL dry Schlenk flask and stirred at 120 °C for 12 h. The mixture was then cooled to room temperature and removed solvents under reduced pressure. The residue was dissolved in $CHCl_3$ (100 mL), then washed with water and brine followed by dried over with anhydrous Na_2SO_4. After removal of solvents under reduced pressure, the residue was purified by silica gel chromatography with eluent (PE:CH_2Cl_2 = 1:1) to give orange solids. Yield: 95%. ^{1}H NMR ($CDCl_3$, 400 MHz, ppm): δ 7.58 (d, J = 7.9 Hz, 1H), 7.34 (d, J = 3.7 Hz, 1H), 7.28 (dd, J = 7.9, 1.3 Hz, 1H), 7.00 (d, J = 1.1 Hz, 1H), 6.85 (d, J = 3.7 Hz, 1H), 3.73 (t, J = 7.4 Hz, 2H), 2.90 (q, J = 7.5 Hz, 2H), 1.70 (s, 2H), 1.39-1.20 (m, 80H), 0.88 (t, J = 6.8 Hz, 6H). ^{13}C NMR ($CDCl_3$, 101 MHz, ppm): δ 182.1, 158.8, 151.7, 151.2, 144.4, 139.7, 126.0, 125.3, 119.9, 115.8, 106.1, 77.3, 77.0, 76.7, 40.5, 37.0, 33.4, 31.9, 30.6, 30.1, 29.7, 29.3, 24.4, 23.7, 22.7, 15.7, 14.1. ESI HRMS calcd. for $C_{54}H_{91}NO_2S$ $(M + H)^+$:818.6843, Found: 818.6858.

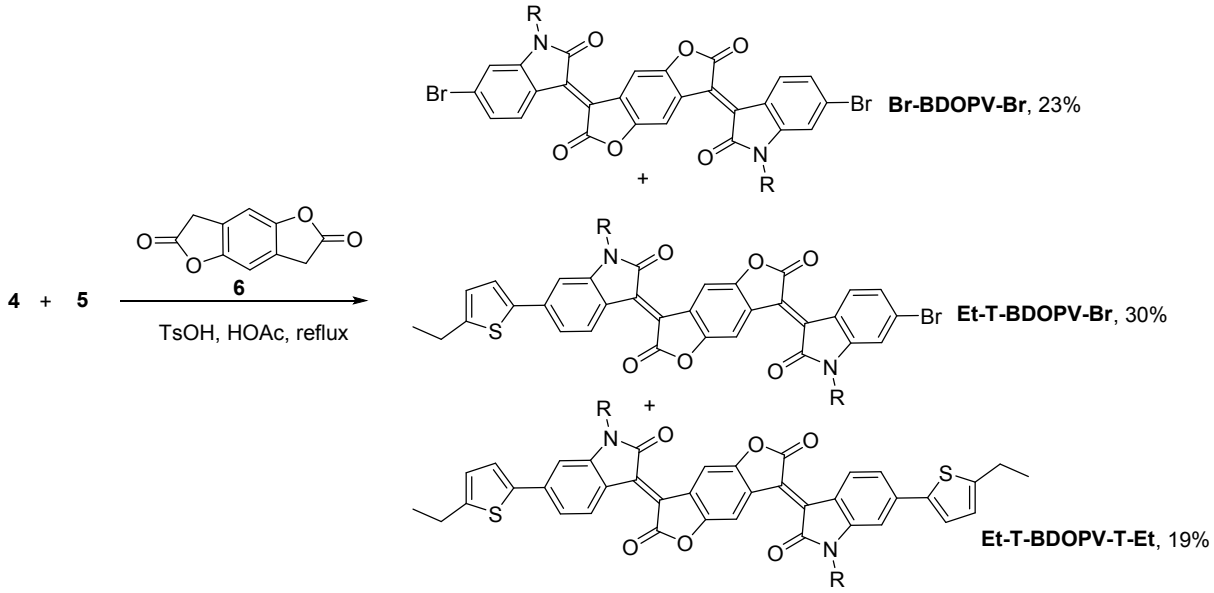

Br-BDOPV-Br, Et-T-BDOPV-Br, Et-T-BDOPV-T-Et: To a solution of compound **4** (1.23 g, 1.6 mmol) and **5** (1.28 g, 1.6 mmol) in acetic acid (30 mL), **6** (0.30 g, 1.6 mmol) and *p*-toluenesulfonic acid monohydrate (0.059 g, 0.31 mmol) was added under N_2 atmosphere. The mixture was heated at 120 °C under N_2 atmosphere for 17 h. The mixture was cooled to room temperature and filtered. After washed with acetic acid and methanol, the residue was purified by silica gel chromatography with eluent (PE:$CHCl_3$

= 3:1) to give the desired compounds as black solids. (**Br-BDOPV-Br**, yield: 23%), (**Et-T- BDOPV-Br**, yield: 30%), and (**Et-T-BDOPV-T-Et**, yield: 19%).

Et-T-BDOPV-Br: ^{1}H NMR ($CDCl_3$, 400 MHz, ppm): δ 9.01 (s, 2H), 8.98 (d, J = 8.5 Hz, 1H), 8.88 (d, J = 8.6 Hz, 1H), 7.23 (d, J = 3.6 Hz, 1H), 7.19-7.13 (m, 2H), 6.87 (d, J = 1.6 Hz, 1H), 6.80 (d, J = 1.0 Hz, 1H), 6.73 (d, J = 3.6 Hz, 1H), 3.75 (dt, J = 25.3, 7.2 Hz, 4H), 2.82 (q, J = 7.4 Hz, 2H), 1.69 (s, 4H), 1.24 (m, 145H), 0.88 (d, J = 6.5 Hz, 12H). ^{13}C NMR ($CDCl_3$, 101 MHz, ppm): δ166.9, 166.6, 146.3, 140.2, 77.3, 77.0, 76.7, 33.6 (s), 31.9, 30.2, 29.7, 29.4, 26.7, 22.7, 14.1. MALDI ESI MS calcd. for $C_{112}H_{177}BrN_2O_6S$ (M^-): 1757.2516, Found: 1757.2500.

Et-T-BDOPV-T-Et: ^{1}H NMR ($CDCl_3$, 400 MHz, ppm): δ 8.99 (d, J = 10.0 Hz, 2H), 7.25 (s, 1H), 7.20 (dd, J = 8.5, 1.4 Hz, 1H), 6.83 (d, J = 1.2 Hz, 1H), 6.75 (d, J = 3.6 Hz, 1H), 3.78 (t, J = 7.0 Hz, 2H), 2.83 (q, J = 7.4 Hz, 2H), 1.72 (s, 2H), 1.23 (d, J = 3.9 Hz, 73H), 0.87 (t, J = 6.8 Hz, 6H). ^{13}C NMR ($C_2D_2Cl_4$, 90 ^{o}C,125 MHz, ppm): δ 166.7, 150.8, 149.5, 146.1, 139.4, 126.0, 124.4, 103.7, 73.6, 73.4, 73.2, 40.0, 36.8, 33.3, 31.3, 30.8, 29.6, 29.1, 28.7, 26.3, 24.2, 23.1, 22.00, 14.8, 13.4. MALDI ESI MS calcd. for $C_{118}H_{184}N_2O_6S_2$ (M^-): 1789.3601, Found: 1789.3567.

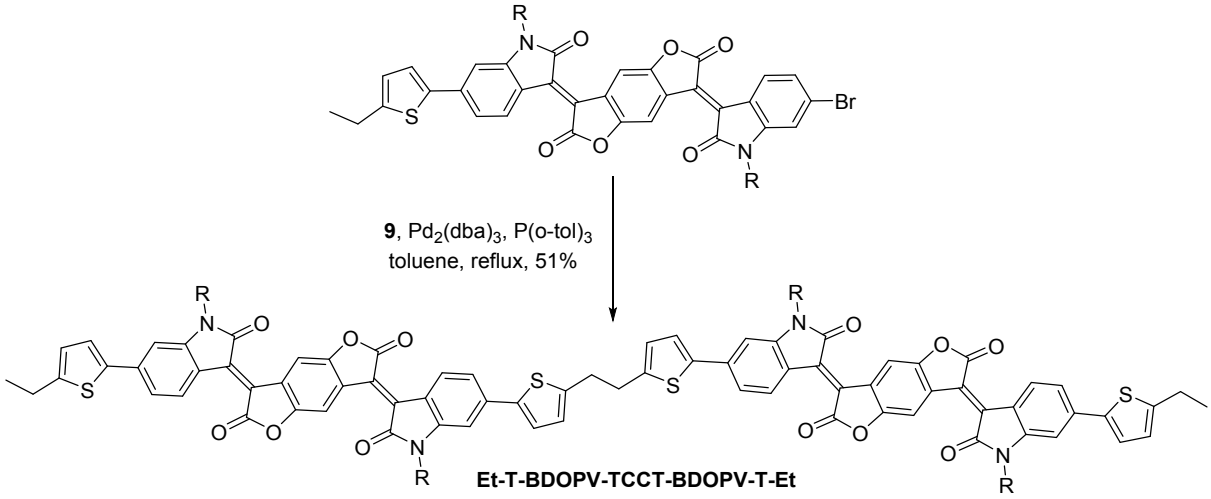

Et-T-BDOPV-TCCT-BDOPV-T-Et: Et-T-BDOPV-Br (123.03 mg, 0.070 mmol), **9** (16.524 mg, 0.032 mmol), $Pd_2(dba)_3$ (1.16 mg), and P(*o*-tol)$_3$ (1.550 mg) were added to a 25 mL dry Schlenk flask and stirred to 120 ^{o}C for 12 h. The mixture was then cooled to room temperature and removed solvents under reduced pressure. The residues were dissolved in $CHCl_3$ (50 mL) and then washed with water and brine, and dried over with anhydrous Na_2SO_4. After removal of the solvents under reduced pressure, the residue was purified by silica gel chromatography with eluent (PE:$CHCl_3$ = 1:1) to give dark blue solids. These solids were separated with gel permeation chromatography, using $CHCl_3$ as mobile phase, to give **Et-T-BDOPV-TCCT-BDOPV-T-Et**. Yield: 51%. ^{1}H NMR ($C_2D_2Cl_4$, 90 ^{o}C, 500 MHz, ppm): δ 8.81 (d, J = 24.6 Hz, 8H), 7.17 – 6.91 (m, 8H), 6.63 (dd, J = 43.3, 23.9 Hz, 8H), 3.81 (s, 8H), 2.71 (d, J = 22.8 Hz, 8H), 1.82 (s, 8H), 1.36 (m, 356H), 0.96 – 0.93 (m, 25H). ^{13}C NMR ($C_2D_2Cl_4$, 90 ^{o}C, 125

MHz, ppm): δ 166.5, 130.5, 124.2, 118.0, 109.8, 73.6, 73.4, 73.2, 40.1, 36.9, 33.4, 31.3, 30.9, 29.6, 29.1, 28.7, 24.3, 22.9, 22.0, 14.5, 13.4. MALDI ESI MS calcd. for $C_{234}H_{362}N_4O_{12}S_4$ (M^-): 3548.6728, Found: 3548.6743.

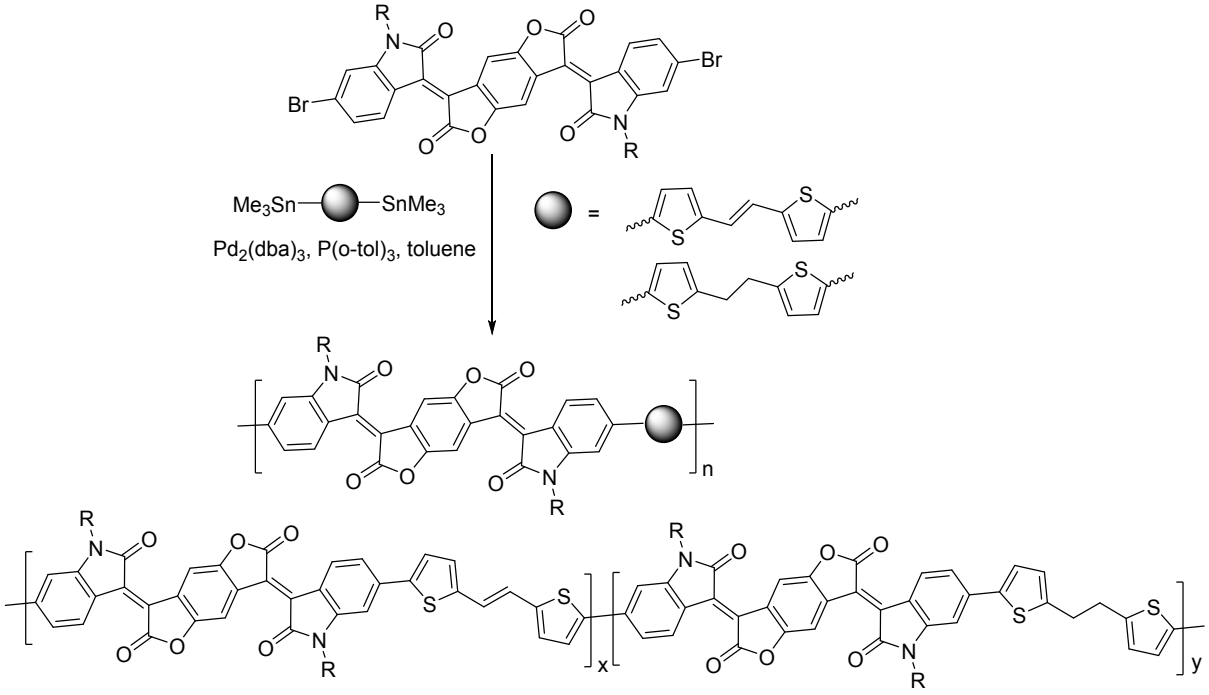

BDOPV-TVT: x = 100%
BDOPV-TVT$_{0.95}$-TCCT$_{0.05}$: x = 95%, y = 5%
BDOPV-TVT$_{0.8}$-TCCT$_{0.2}$: x = 80%, y = 20%
BDOPV-TVT$_{0.5}$-TCCT$_{0.5}$: x = 50%, y = 50%
BDOPVTCCT: y = 100%

General Procedure for the Stille Polymerization:

BDOPV-TVT: **BDOPV** (98.2 mg, 0.0568 mmol), (*E*)-trimethyl(5-(3-(((trimethylstannyl)methyl)thio)prop-1-en-1-yl)thiophen-2-yl)stannane (29.4 mg, 0.0568 mmol), $Pd_2(dba)_3$ (2.08 mg, 4 mol%), P(*o*-tol)$_3$ (2.77 mg, 16 mol%), and 8 mL of toluene were added to a Schlenk flask. The flask was charged with N_2 through a freeze-pump-thaw cycle for three times. After 2 h at 120 ^oC, *N*,*N'*-diethylphenylazothioformamide (10 mg) was then added to the mixture and then further stirred for 1 h to remove any residual catalyst before being precipitated into methanol (200 mL). The precipitate was filtered through a nylon filter and purified via Soxhlet extraction with acetone, hexane, and chloroform. The chloroform solution was then concentrated by evaporation and precipitated into methanol (200 mL) and filtered off to afford dark solids (96 mg, yield 96%).

BDOPV-TCCT: The synthetic procedure is similar to that of BDOPV-TVT. (Yield: 95%).

BDOPV-TVT$_{0.95}$-TCCT$_{0.05}$: **BDOPV** (95.1 mg, 0.0550 mmol), (*E*)-trimethyl(5-(3-(((trimethylstannyl)methyl)thio)prop-1-en-1-yl)thiophen-2-yl)stannane (27.1 mg,

0.0522 mmol), 1,2-bis(5-(trimethylstannyl)thiophen-2-yl)ethane (1.4 mg, 0.00275 mmol), $Pd_2(dba)_3$ (2.01 mg, 4 mol%), P(*o*-tol)$_3$ (2.68 mg, 16 mol%), and 8 mL of toluene were added to a Schlenk flask. The flask was charged with nitrogen through a freeze-pump-thaw cycle for three times. Afterr 2 h at 120 °C, *N*,*N'*-diethylphenylazothioformamide (10 mg) was then added to the mixture and then further stirred for 1 h to remove any residual catalyst before being precipitated into methanol (200 mL). The precipitate was filtered through a nylon filter and purified via Soxhlet extraction with acetone, hexane, and chloroform. The chloroform solution was then concentrated by evaporation and precipitated into methanol (200 mL) and filtered off to afford dark solids (80 mg, yield 82%).

BDOPV-TVT$_{0.8}$-TCCT$_{0.2}$: The synthetic procedure is similar to that of BDOPV-TVT$_{0.95}$-TCCT$_{0.05}$. (Yield: 80%).

BDOPV-TVT$_{0.5}$-TCCT$_{0.5}$: The synthetic procedure is similar to that of BDOPV-TVT$_{0.95}$-TCCT$_{0.05}$. (Yield: 91%).

3. ^{1}H and ^{13}C NMR spectra of new compounds

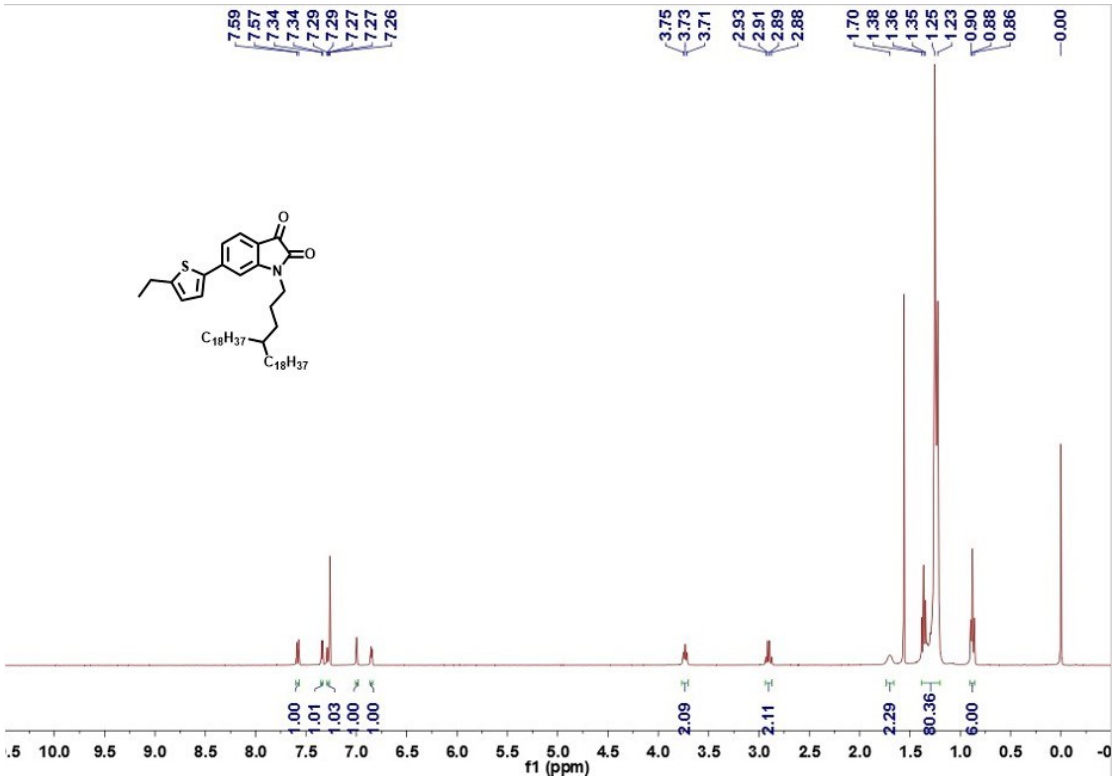

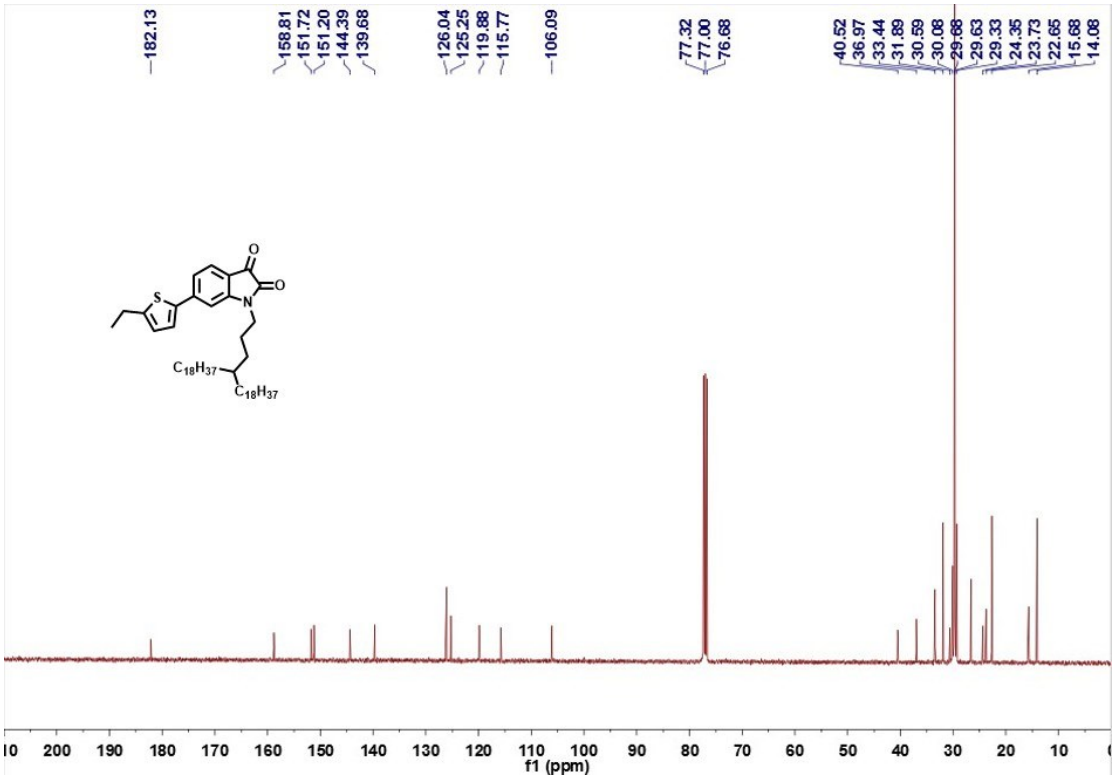

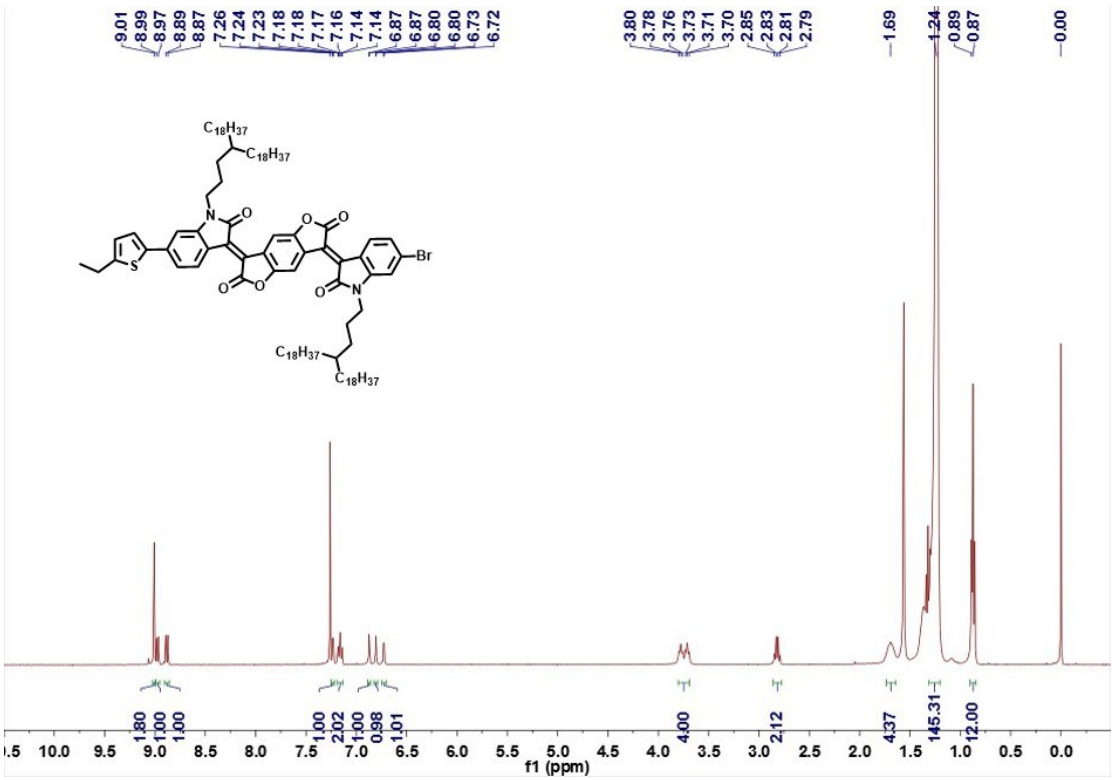
9.01
8.99
8.97
8.89
8.87
7.26
7.24
7.23
7.18
7.18
7.17
7.16
7.14
7.14
6.87
6.87
6.80
6.80
6.73
6.72
3.80
3.78
3.76
3.73
3.71
3.70
2.85
2.83
2.81
2.79
1.69
1.24
0.89
0.87
0.00
1.80
1.00
1.00
1.00
2.02
1.00
0.98
1.01
4.00
2.12
4.37
145.31
12.00
f1 (ppm)

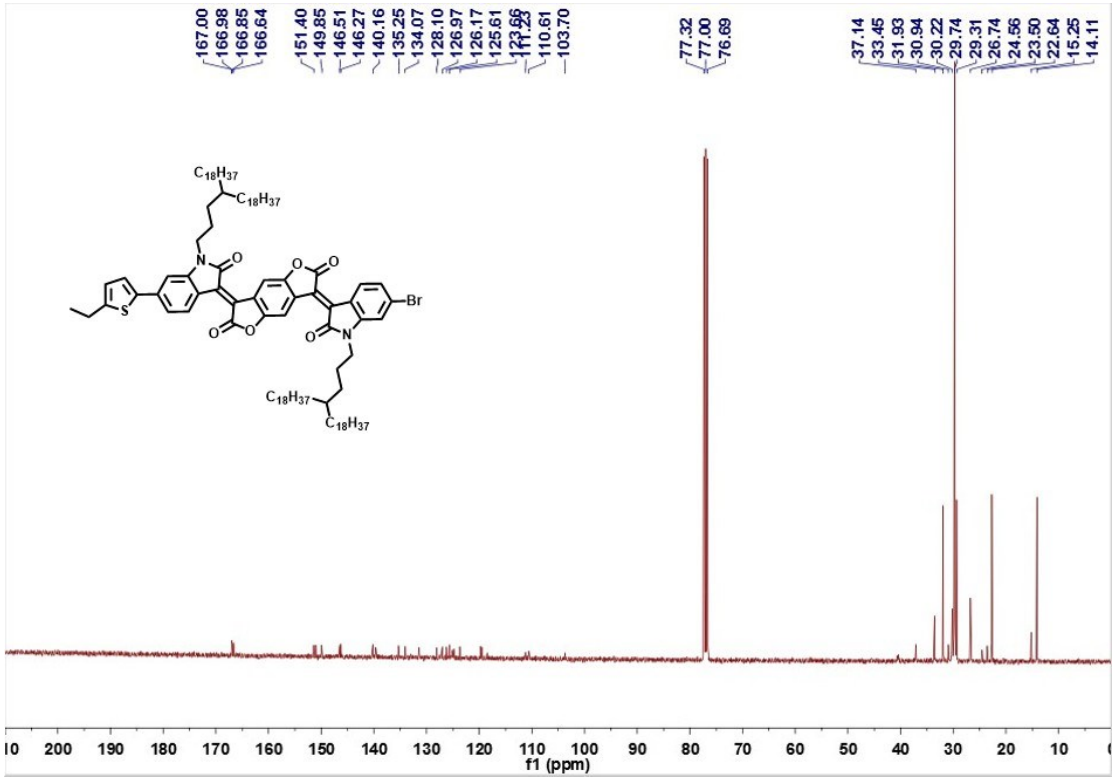
167.00
166.98
166.85
166.64
151.40
149.85
146.51
146.27
140.16
135.25
134.07
128.10
126.97
126.17
125.61
110.61
103.70
77.32
77.00
76.69
37.14
33.45
31.93
30.94
30.22
29.74
29.31
26.74
24.56
23.50
22.64
15.25
14.11
f1 (ppm)

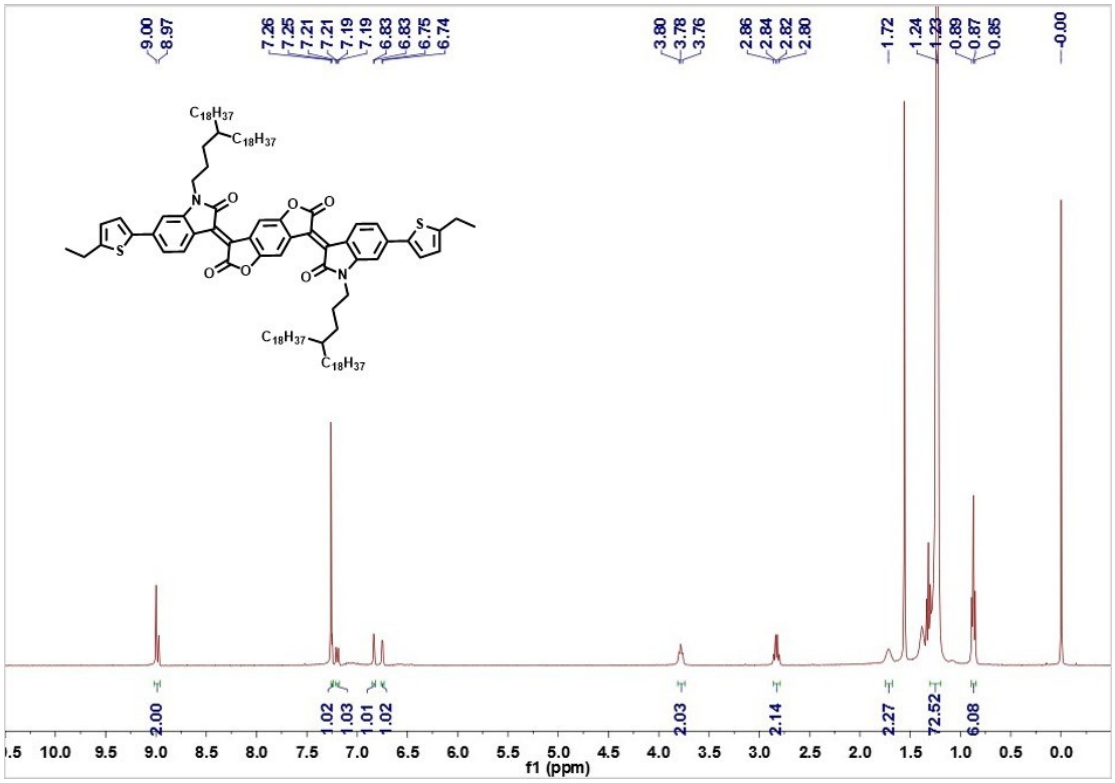
9.00
8.97
7.26
7.25
7.21
7.21
7.19
7.19
6.83
6.75
6.74
3.80
3.78
3.76
2.86
2.84
2.82
2.80
1.72
1.24
1.23
0.89
0.87
0.85
0.00
2.00
1.02
1.03
1.01
1.02
2.03
2.14
2.27
72.52
6.08
f1 (ppm)

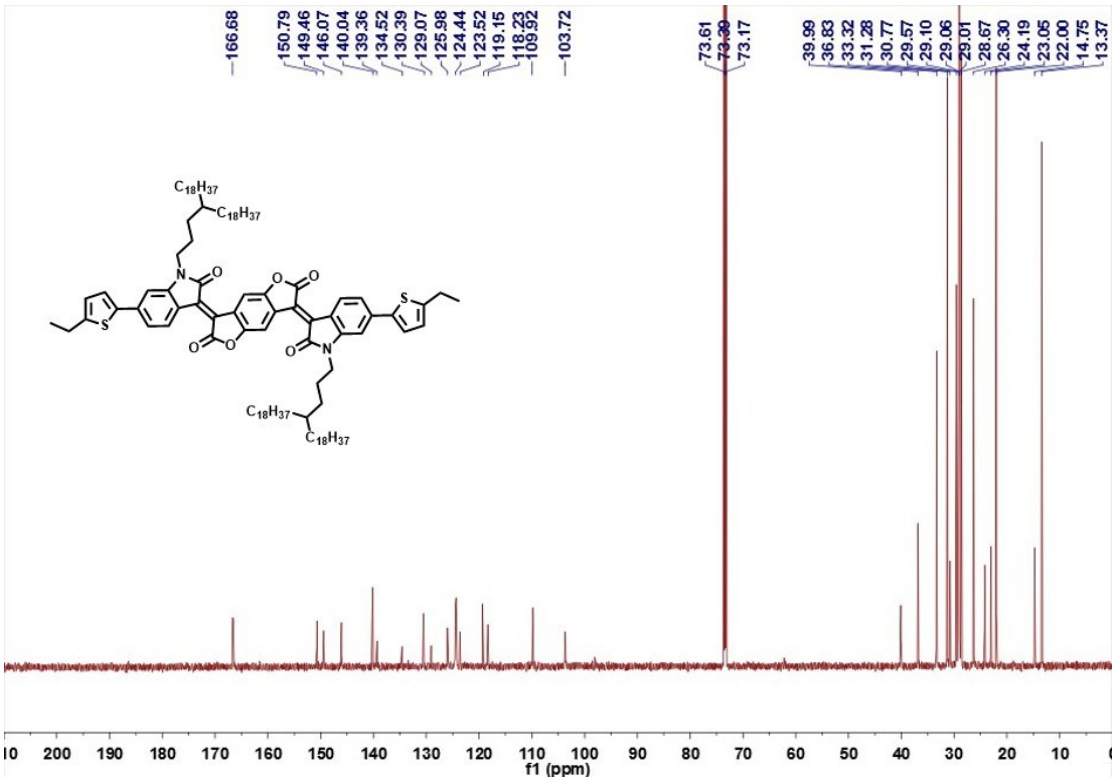
166.68
150.79
149.46
146.07
140.04
139.36
134.52
130.39
129.07
125.98
124.44
123.52
119.15
118.23
109.52
103.72
73.61
73.30
73.17
39.99
36.83
33.32
31.28
30.77
29.57
29.10
29.06
29.01
28.67
26.30
24.19
23.05
22.00
14.75
13.37
f1 (ppm)

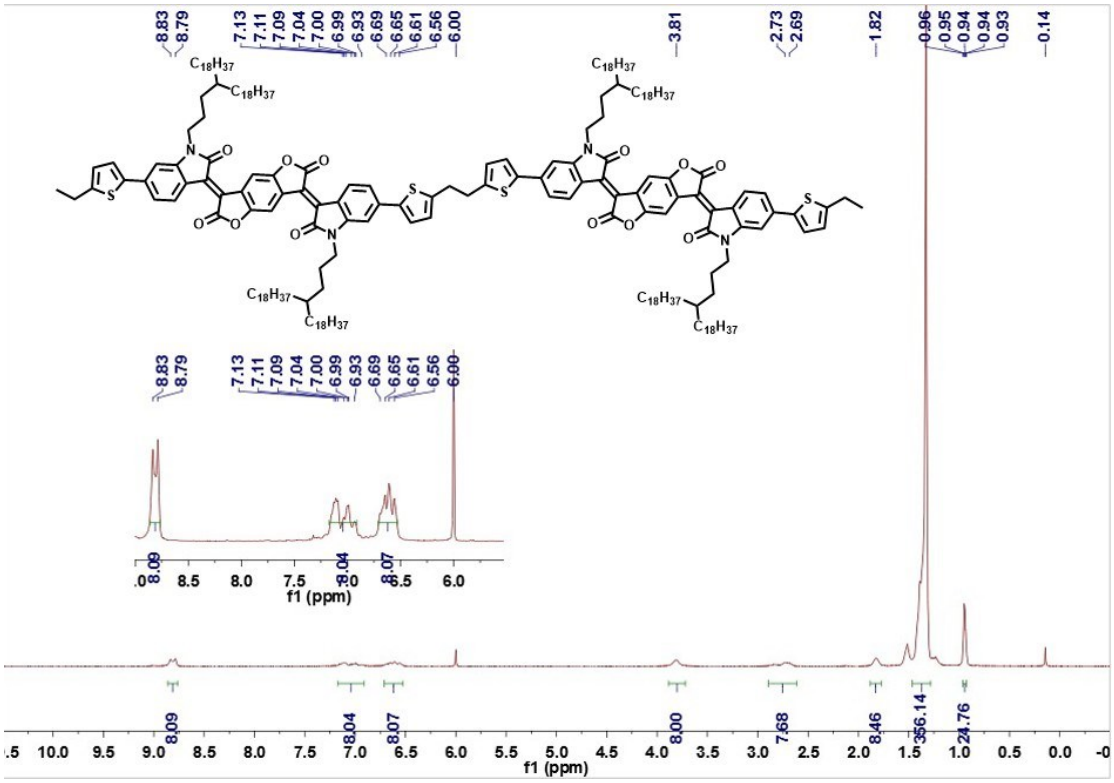
8.83
8.79
7.13
7.11
7.09
7.04
7.00
6.99
6.93
6.69
6.65
6.61
6.56
6.00
3.81
2.73
2.69
1.82
0.96
0.95
0.94
0.94
0.93
0.14
f1 (ppm)

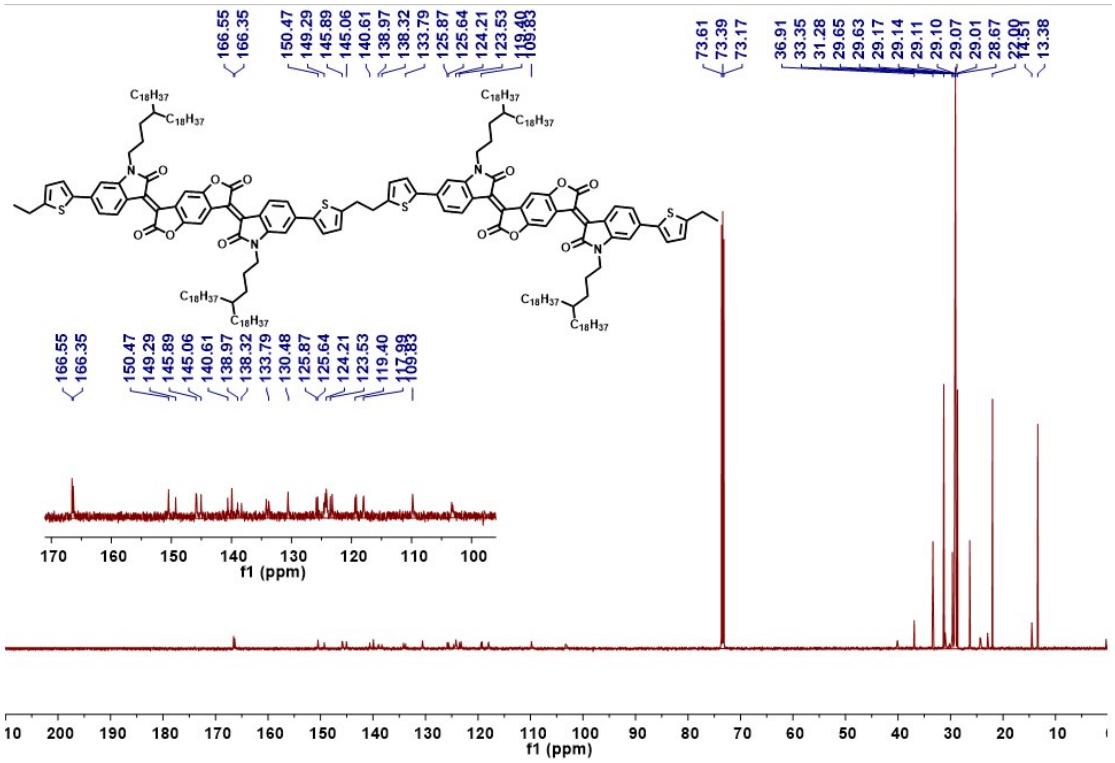
166.55
166.35
150.47
149.29
145.89
145.06
140.61
138.97
138.32
133.79
125.87
125.64
124.21
123.53
119.40
73.61
73.39
73.17
36.91
33.35
31.28
29.65
29.63
29.17
29.14
29.11
29.10
29.07
29.01
28.67
13.38
f1 (ppm)

4. Figures S1-8 and Tables S1-3

a)

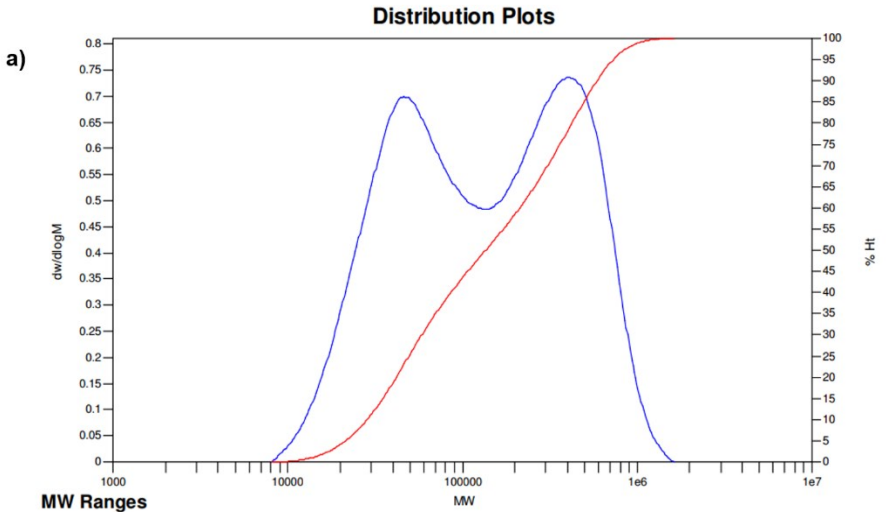

b)

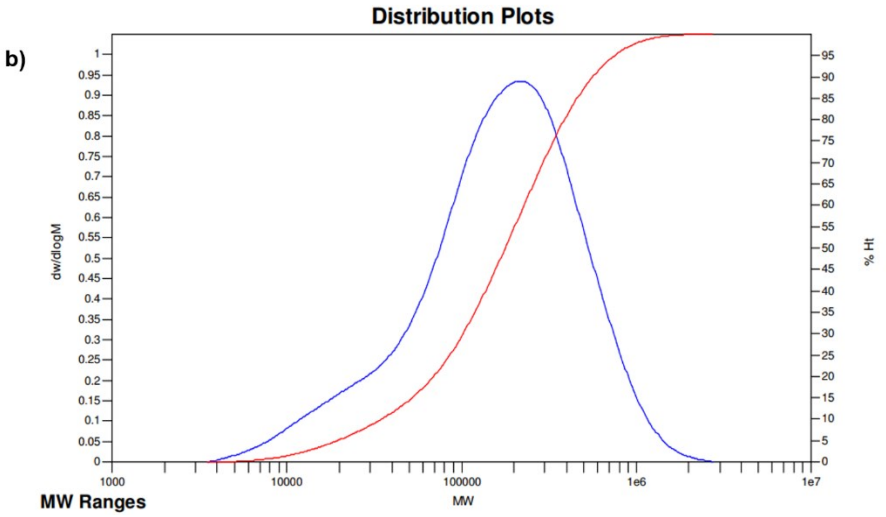

c)

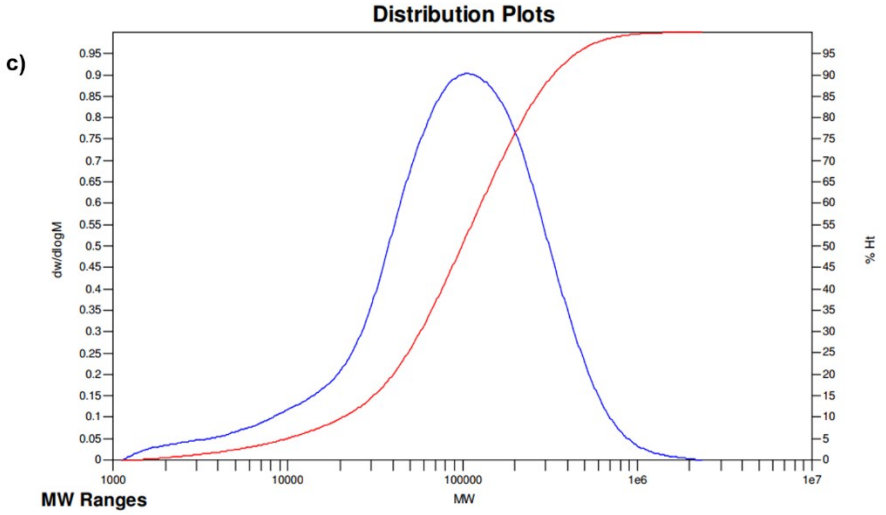

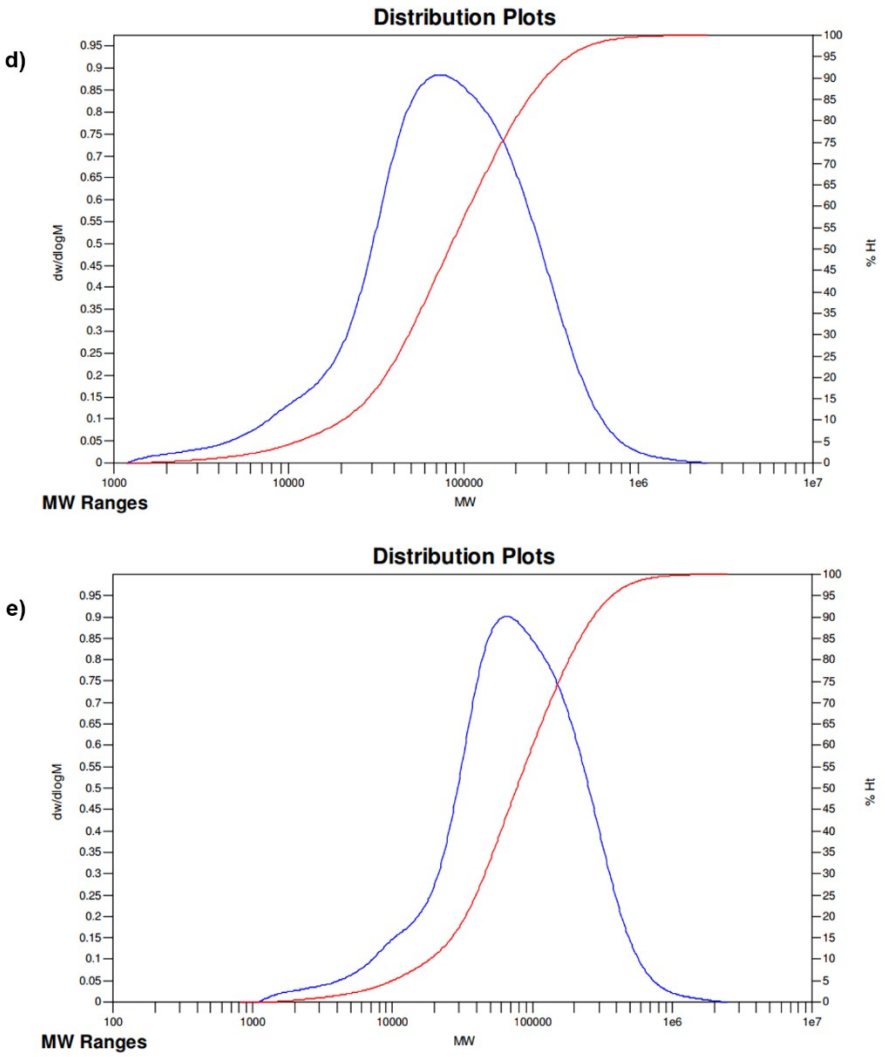

Figure S1. High temperature gel permeation chromatography (GPC) plots of BDOPV-TVT (**a**), BDOPV-$TVT_{0.95}$-$TCCT_{0.05}$ (**b**), BDOPV-$TVT_{0.8}$-$TCCT_{0.2}$ (**c**), BDOPV-$TVT_{0.5}$-$TCCT_{0.5}$ (**d**), BDOPV-TCCT (**e**).

Table S1. Molecular weights and distribution of the polymers [a)]

Polymer	M_p	M_n	M_v	M_w	M_z	$M_z + 1$	*PDI*
BDOPV-TVT	65390	34843	105210	121162	284597	573628	3.4774
BDOPV-$TVT_{0.95}$-$TCCT_{0.05}$	72599	38648	112786	129721	300660	592452	3.3565
BDOPV-$TVT_{0.8}$-$TCCT_{0.2}$	107057	36966	128693	147370	321084	578943	3.9866
BDOPV-$TVT_{0.5}$-$TCCT_{0.5}$	219300	78914	222216	251790	502044	799584	3.1907
BDOPV- TCCT	404619	70829	201055	233749	479215	652635	3.3002

[a)] GPC versus polystyrene standards in 1,2,4-trichlorobenzene at 150 °C.

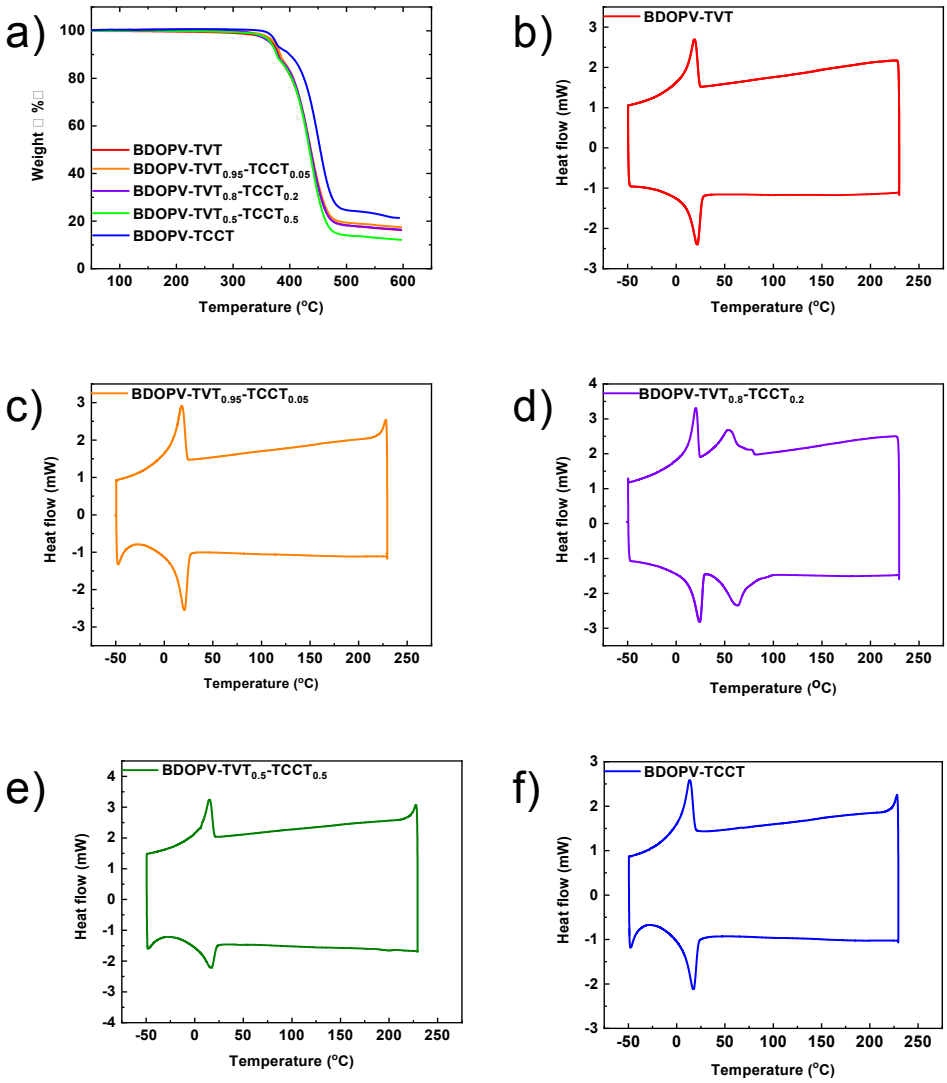

Figure S2. Thermal gravity analysis (TGA) (**a**) and differential scanning calorimeter traces (DSC) of BDOPV-TVT (**b**), BDOPV-TVT$_{0.95}$-TCCT$_{0.05}$ (**c**), BDOPV-TVT$_{0.8}$-TCCT$_{0.2}$ (**d**), BDOPV-TVT$_{0.5}$-TCCT$_{0.5}$ (**e**) and BDOPV-TCCT (**f**).

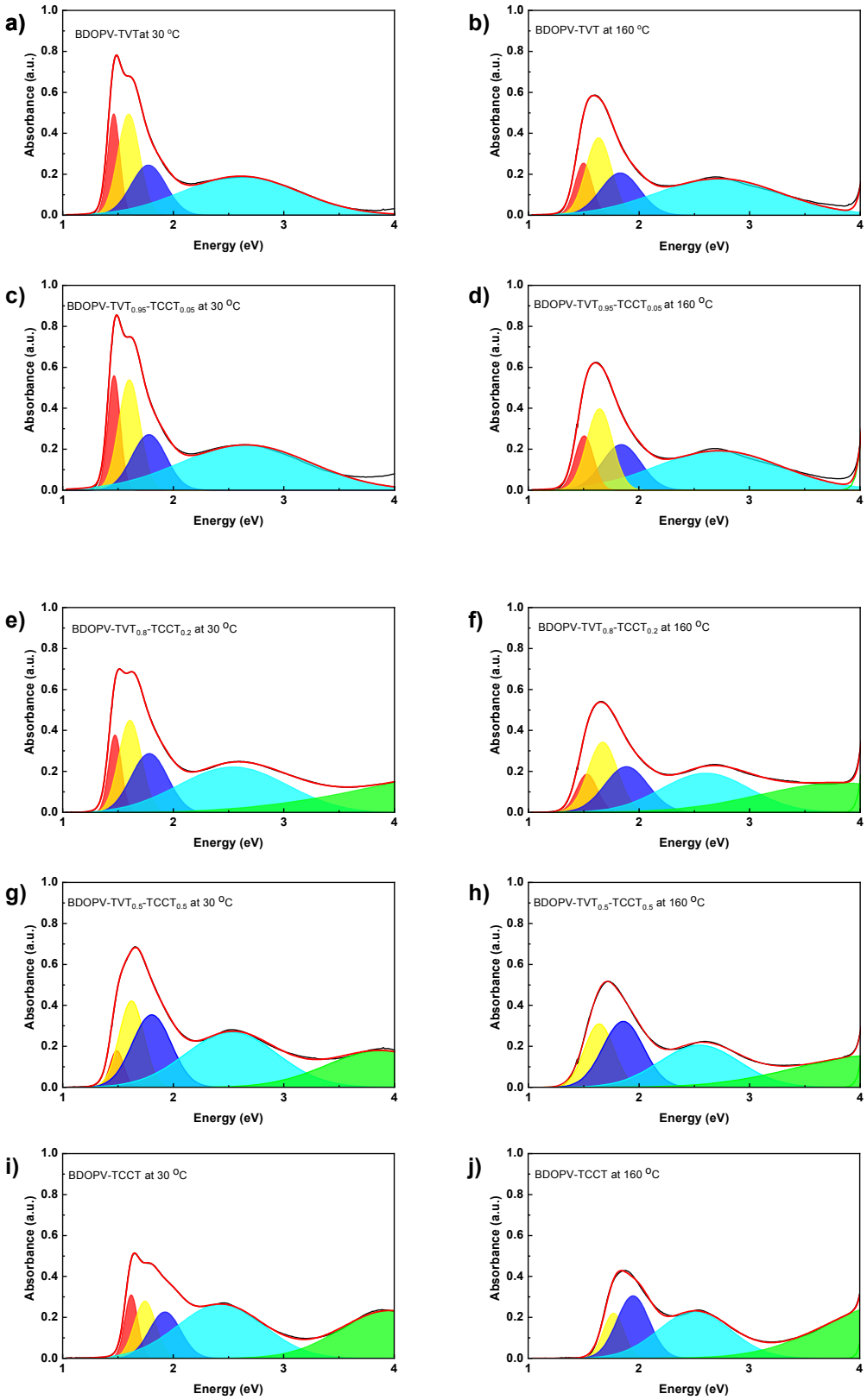

Figure S3. Peak fitting at 30 °C and 160 °C for BDOPV-TVT (**a**, **b**), BDOPV-TVT$_{0.95}$-TCCT$_{0.05}$ (**c**, **d**), BDOPV-TVT$_{0.8}$-TCCT$_{0.2}$ (**e**, **f**), BDOPV-TVT$_{0.5}$-TCCT$_{0.5}$ (**g**, **h**) and BDOPV-TCCT (**i**, **j**).

Table S2. Polymer peak fitting of location and intensity

Polymer	30 °C		160 °C	
	λ (nm)	A_1/A_2	λ (nm)	A_1/A_2
BDOPV-TVT	848, 776	1.00	827, 758	0.67
BDOPV-TVT$_{0.95}$-TCCT$_{0.05}$	846, 774	1.04	823, 753	0.67
BDOPV-TVT$_{0.8}$-TCCT$_{0.2}$	841, 771	0.84	811, 742	0.54
BDOPV-TVT$_{0.5}$-TCCT$_{0.5}$	832, 764	0.42	756	---
BDOPV- TCCT	765, 711	1.11	699	---

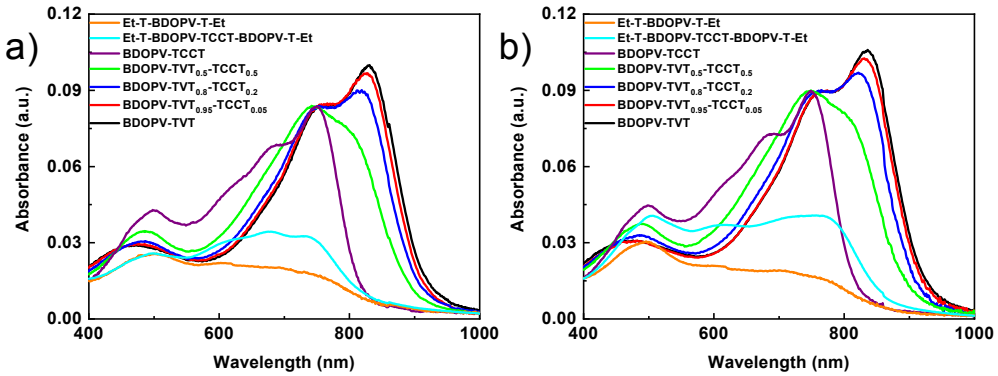

Figure S4. UV-vis-NIR absorption spectra of intrinsic thin films (**a**) and annealled thin films at 180 °C (**b**).

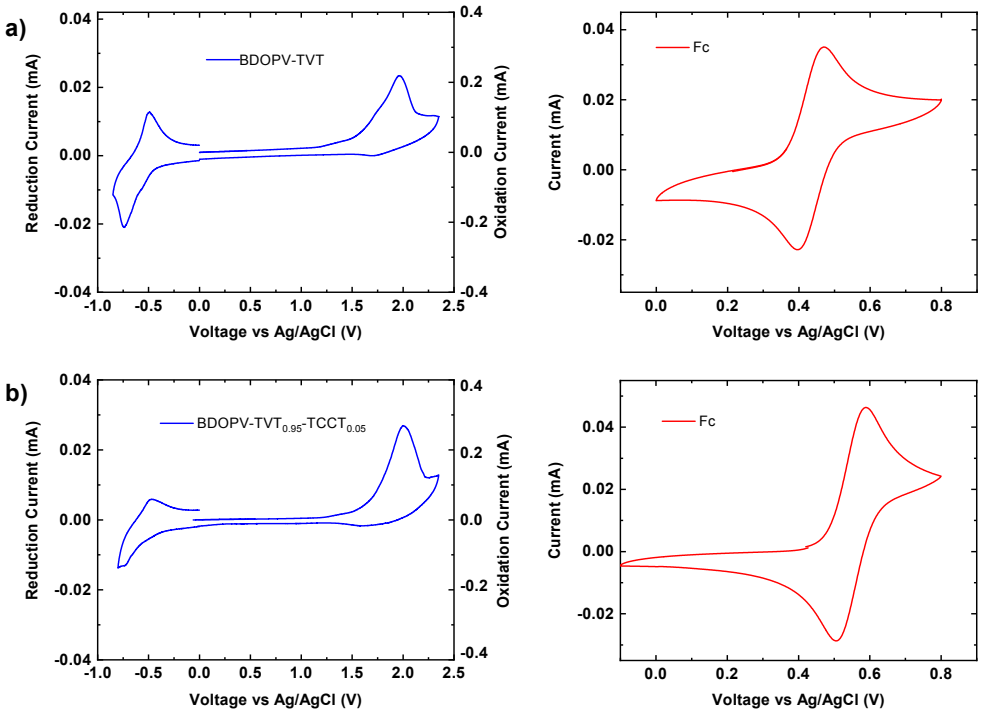

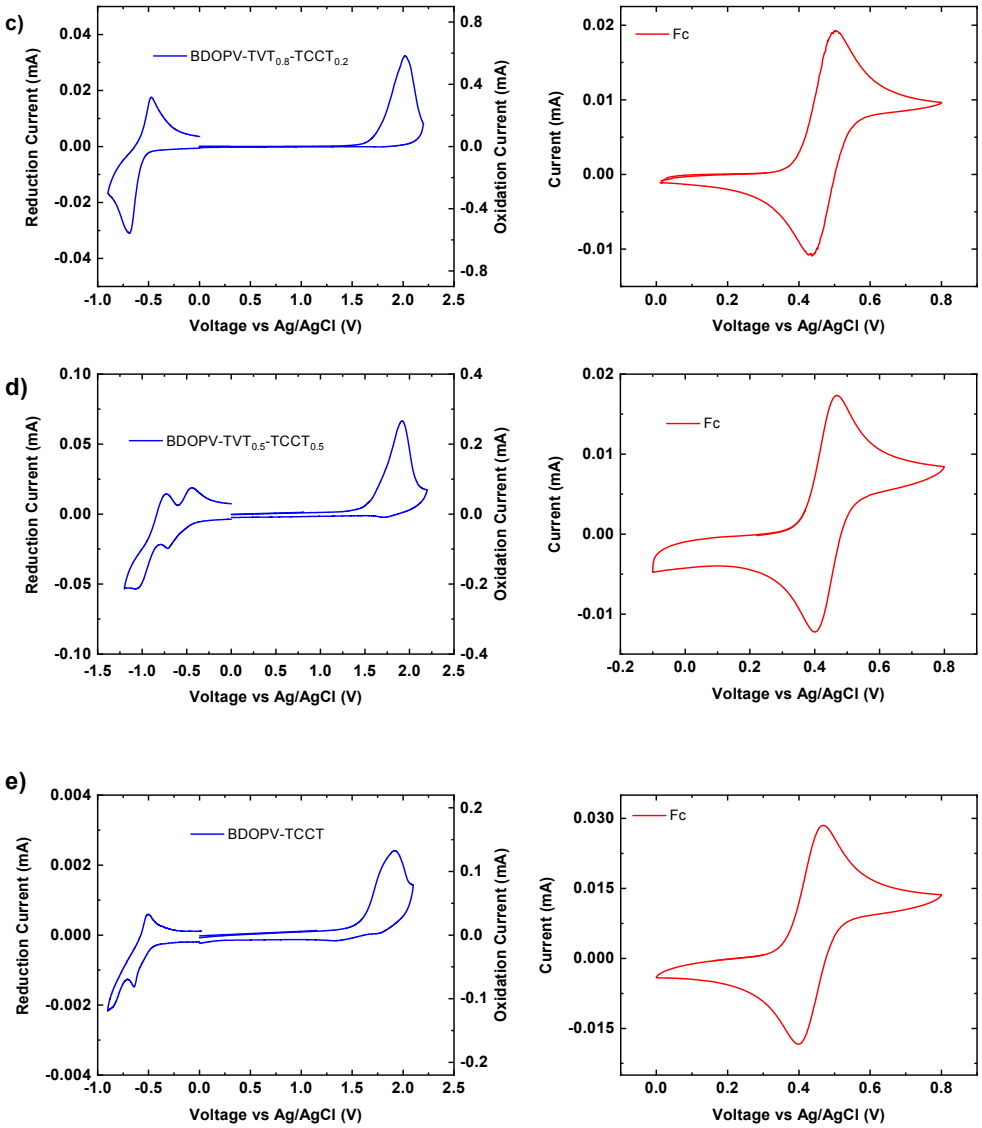

Figure S5. Cyclic voltammetry of polymers and ferrocene: BDOPV-TVT (**a**), BDOPV-TVT$_{0.95}$-TCCT$_{0.05}$ (**b**), BDOPV-TVT$_{0.8}$-TCCT$_{0.2}$ (**c**), BDOPV-TVT$_{0.5}$-TCCT$_{0.5}$ (**d**), BDOPV-TCCT (**e**).

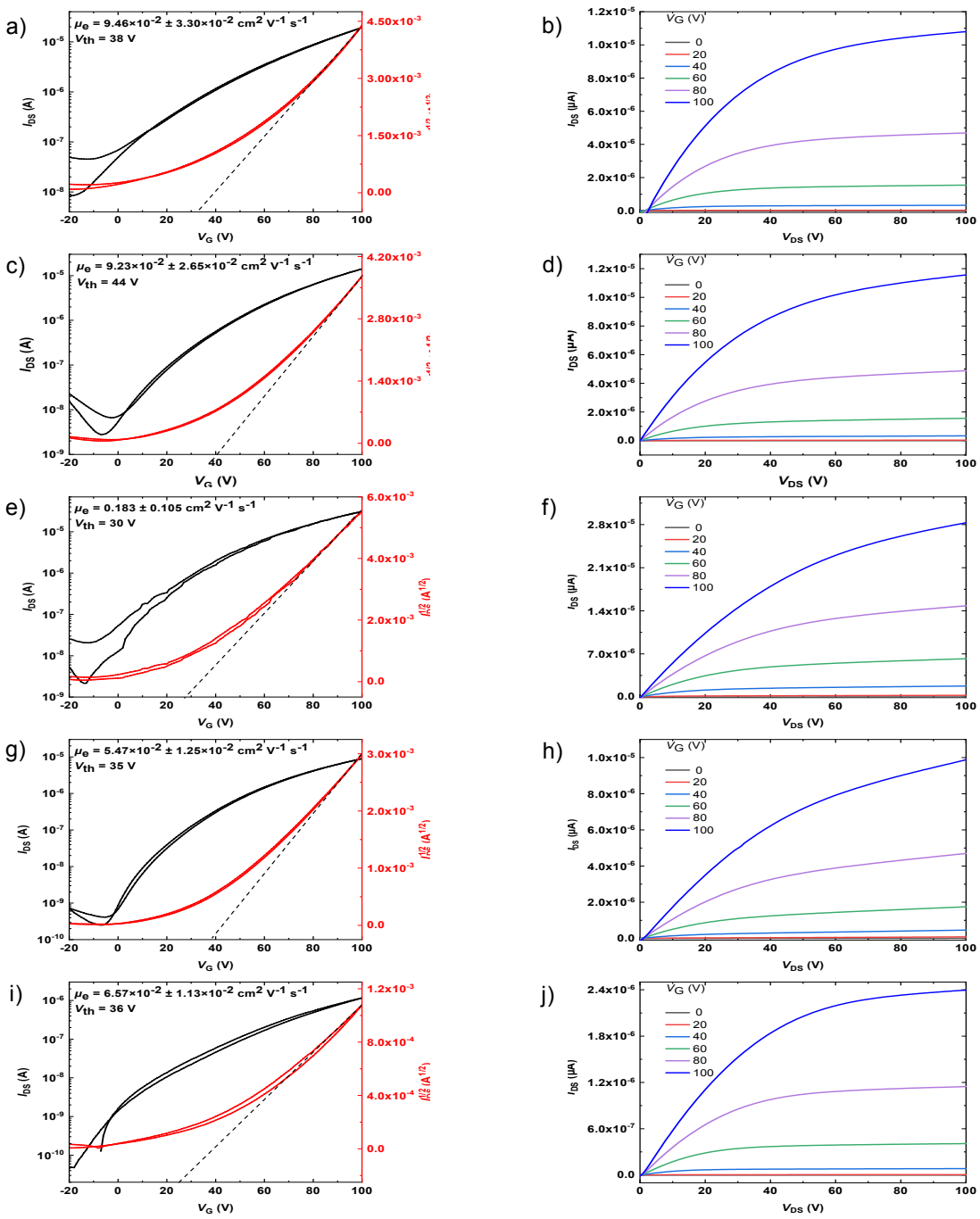

Figure S6. Transfer and output curves for BDOPV-TVT (**a**, **b**), BDOPV-TVT$_{0.95}$-TCCT$_{0.05}$ (**c**, **d**), BDOPV-TVT$_{0.8}$-TCCT$_{0.2}$ (**e**, **f**), BDOPV-TVT$_{0.5}$-TCCT$_{0.5}$ (**g**, **h**) and BDOPV-TCCT (**i**, **j**).

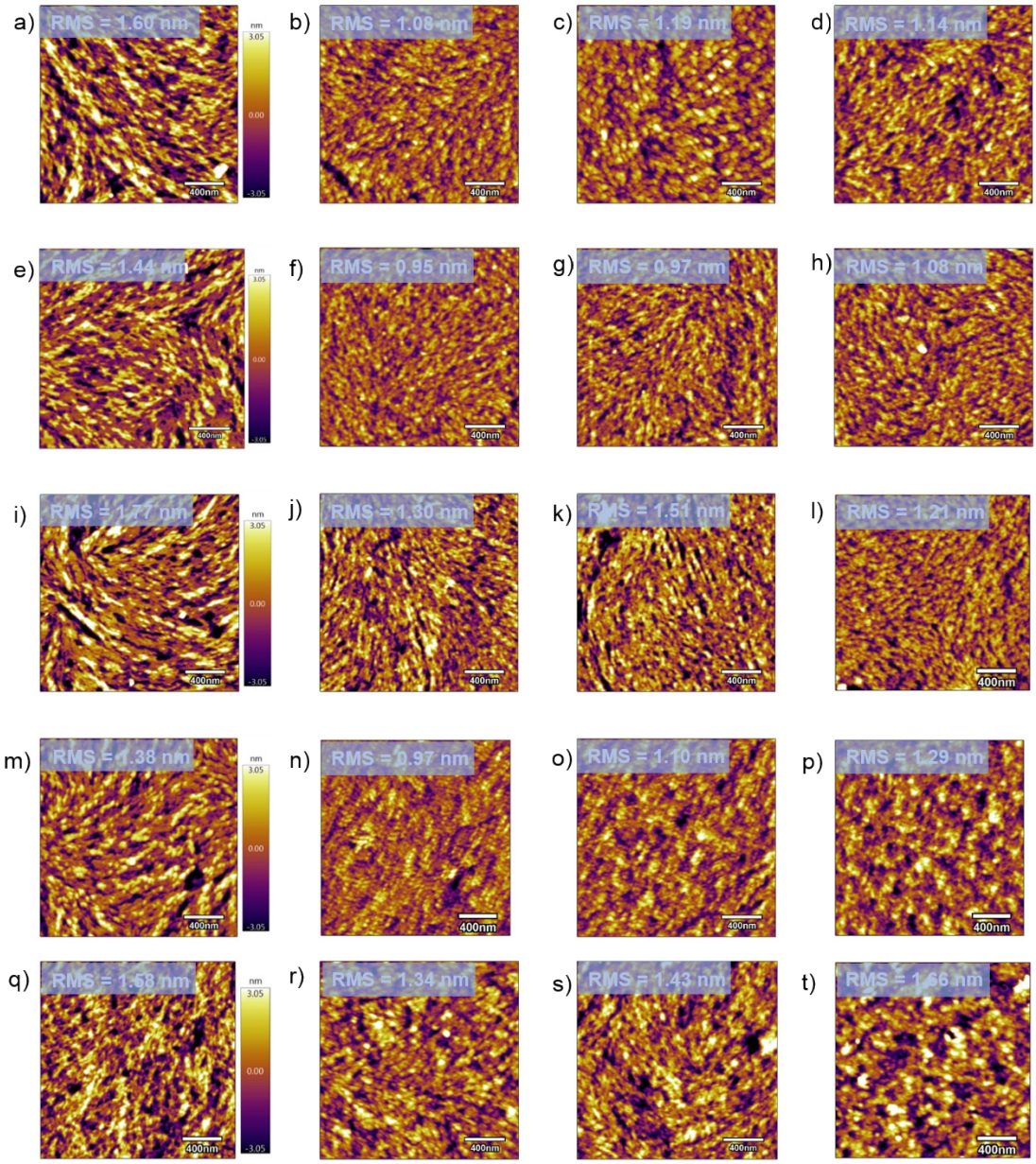

Figure S7. AFM height images of intrinsic films of BDOPV-TVT (**a**), BDOPV-$TVT_{0.95}$-$TCCT_{0.05}$ (**e**), BDOPV-$TVT_{0.8}$-$TCCT_{0.2}$ (**i**), BDOPV-$TVT_{0.5}$-$TCCT_{0.5}$ (**m**), and BDOPV-TCCT (**q**) and the corresponding doped films with 16 mol% *N*-DMBI **(b, f, j, n, r)**, 30 mol% **(c, g, k, o, s)** and 45 mol% **(d, h, i, p, t)** *N*-DMBI.

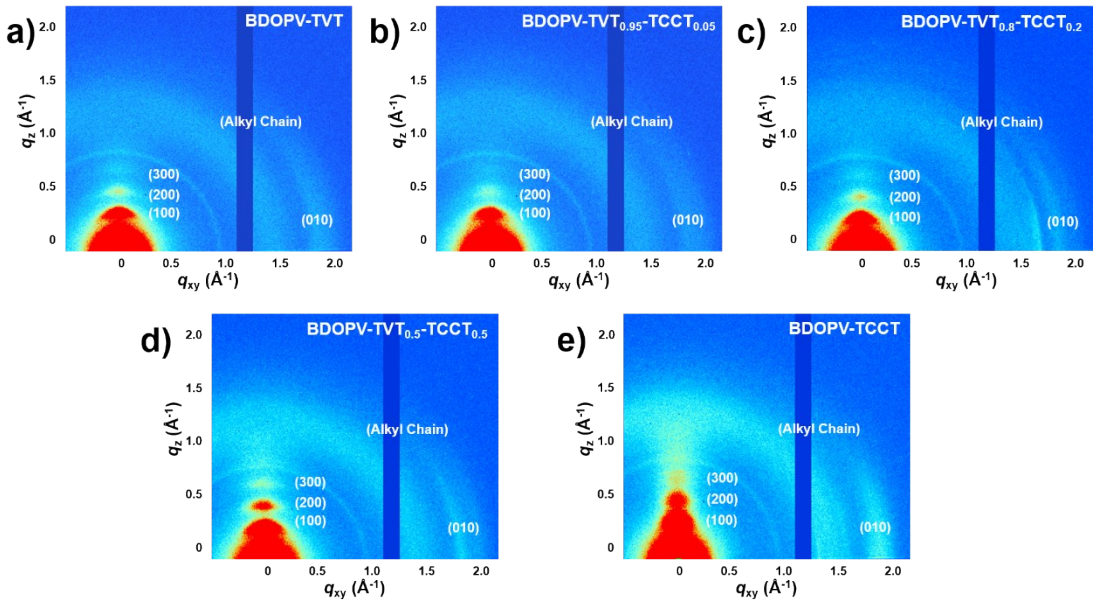

Figure S8. 2D GIWAXS patterns of BDOPV-TVT (**a**), BDOPV-TVT$_{0.95}$-TCCT$_{0.05}$ (**b**), BDOPV-TVT$_{0.8}$-TCCT$_{0.2}$ (**c**), BDOPV-TVT$_{0.5}$-TCCT$_{0.5}$ (**d**) and BDOPV-TCCT (**e**) thin films.

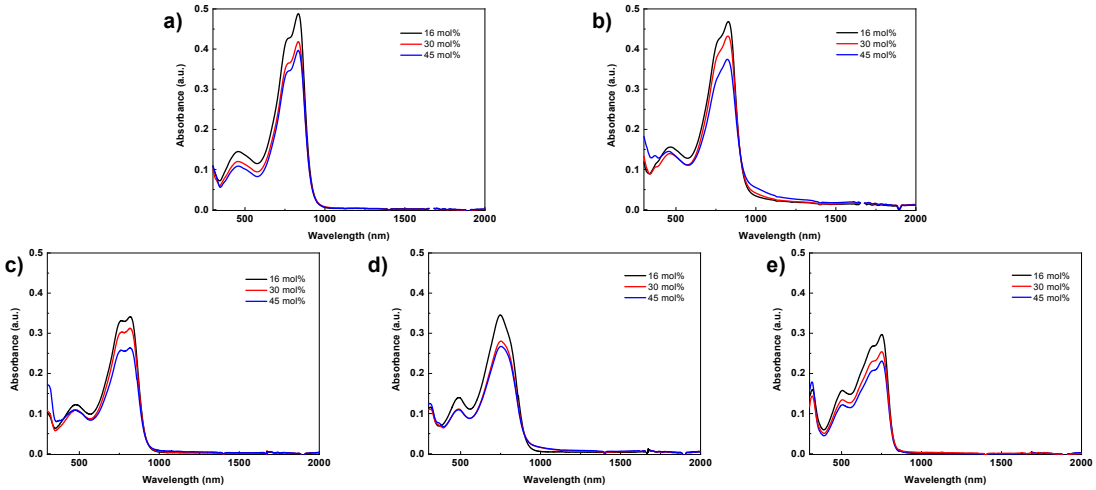

Figure S9. UV-*vis*-NIR absorption spectra of doped solutions with (16 mol%, 30 mol% and 45 mol%) *N*-DMBI for BDOPV-TVT (**a**), BDOPV-TVT$_{0.95}$-TCCT$_{0.05}$ (**b**), BDOPV-TVT$_{0.8}$-TCCT$_{0.2}$ (**c**), BDOPV-TVT$_{0.5}$-TCCT$_{0.5}$ (**d**) and BDOPV-TCCT (**e**).

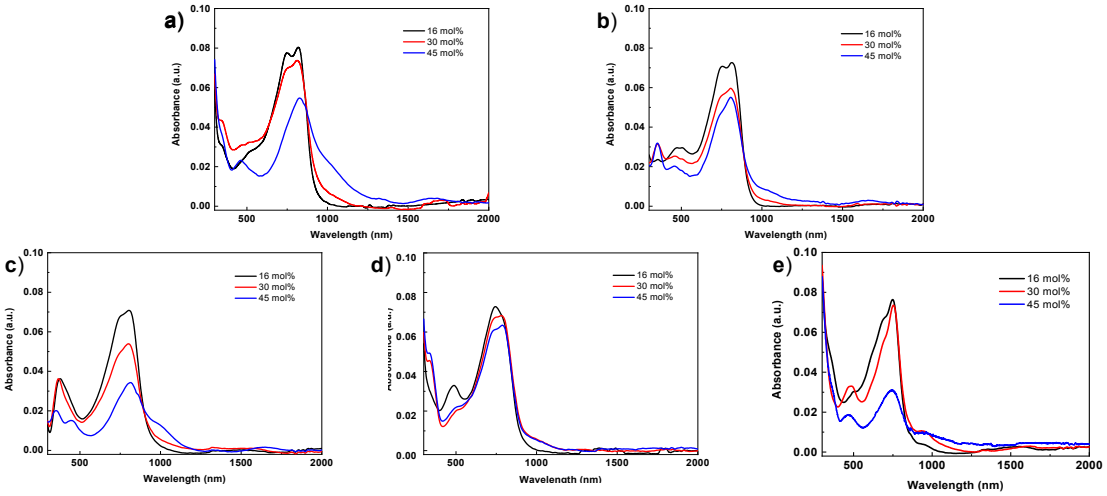

Figure S10. UV-*vis*-NIR absorption spectra of doped films with (16 mol%, 30 mol% and 45 mol%) *N*-DMBI for BDOPV-TVT (**a**), BDOPV-TVT$_{0.95}$-TCCT$_{0.05}$ (**b**), BDOPV-TVT$_{0.8}$-TCCT$_{0.2}$ (**c**), BDOPV-TVT$_{0.5}$-TCCT$_{0.5}$ (**d**) and BDOPV-TCCT (**e**).

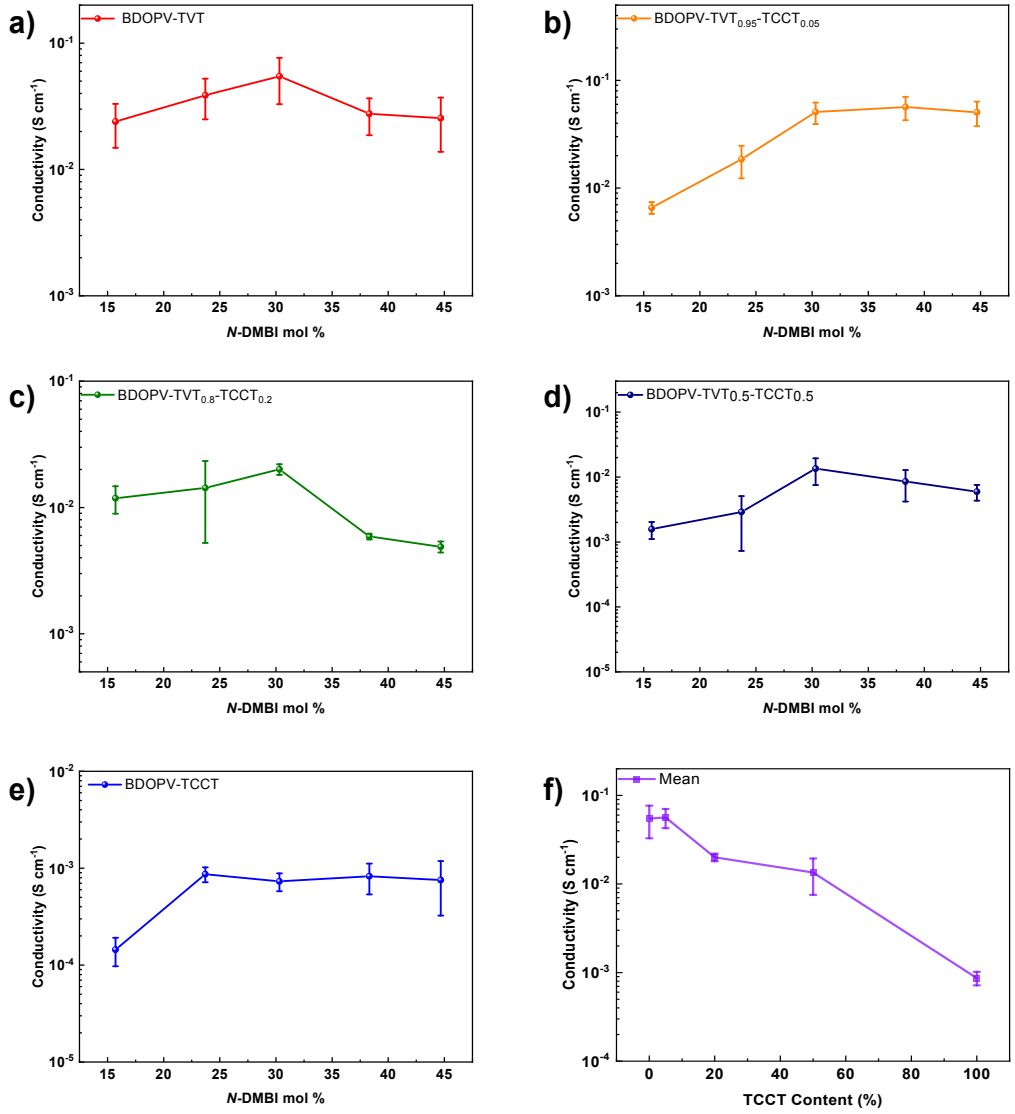

Figure S11. Electronic conductivities of the doped polymers at different concentrations

of the dopant *N*-DMBI (**a-e**), electronic conductivities of 30 mol% *N*-DMBI doped polymers with different ratios of TCCT (**f**).

Table S3. d-d Stacking distances, π-π stacking distances and coherence length of five intrinsic polymers.

Polymer	d-d (Å)	π-π (Å)	Coherence Length (Å)
BDOPV-TVT	29.77	3.51	144.5
BDOPV-TVT$_{0.95}$-TCCT$_{0.05}$	29.04	3.49	118.1
BDOPV-TVT$_{0.8}$-TCCT$_{0.2}$	29.92	3.42/3.62	112.5
BDOPV-TVT$_{0.5}$-TCCT$_{0.5}$	29.51	3.42/3.65	125.5
BDOPV-TCCT	30.75	3.51	100.8

Obtained from their respective thin films fabricated on SiO_2/Si after annealing at 180 °C for 10 min.

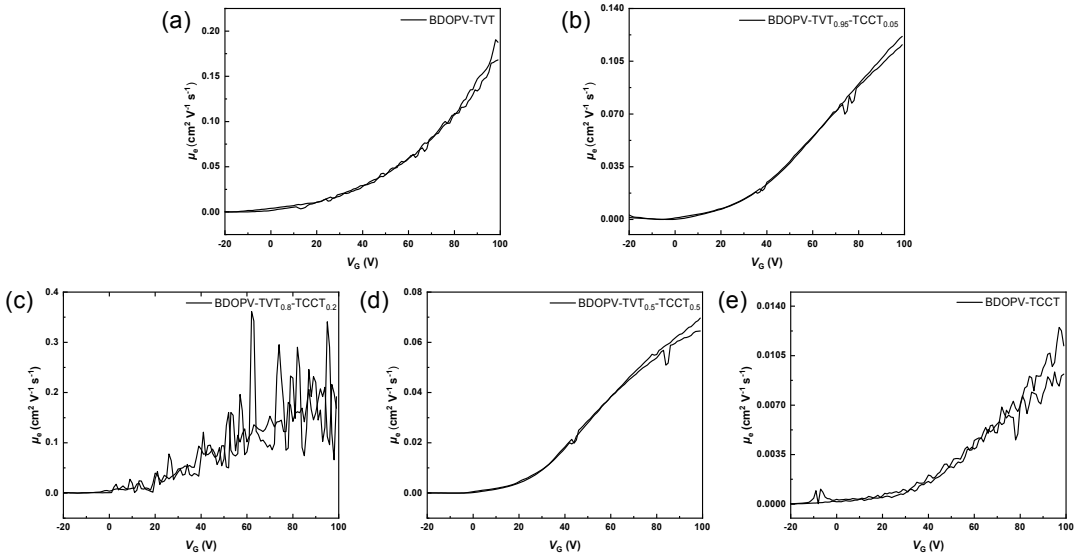

Fig. S12. Mobilities as a function of gate voltage. a) BDOPV-TVT, b) BDOPV-TVT$_{0.95}$-TCCT$_{0.05}$, c) BDOPV-TVT$_{0.8}$-TCCT$_{0.2}$, d) BDOPV-TVT$_{0.5}$-TCCT$_{0.5}$, e) BDOPV- TCCT. The mobilities are calculated from the local slopes of the square root of the transfer curves at saturation regime ($I_{DS}^{1/2}$ versus V_G).

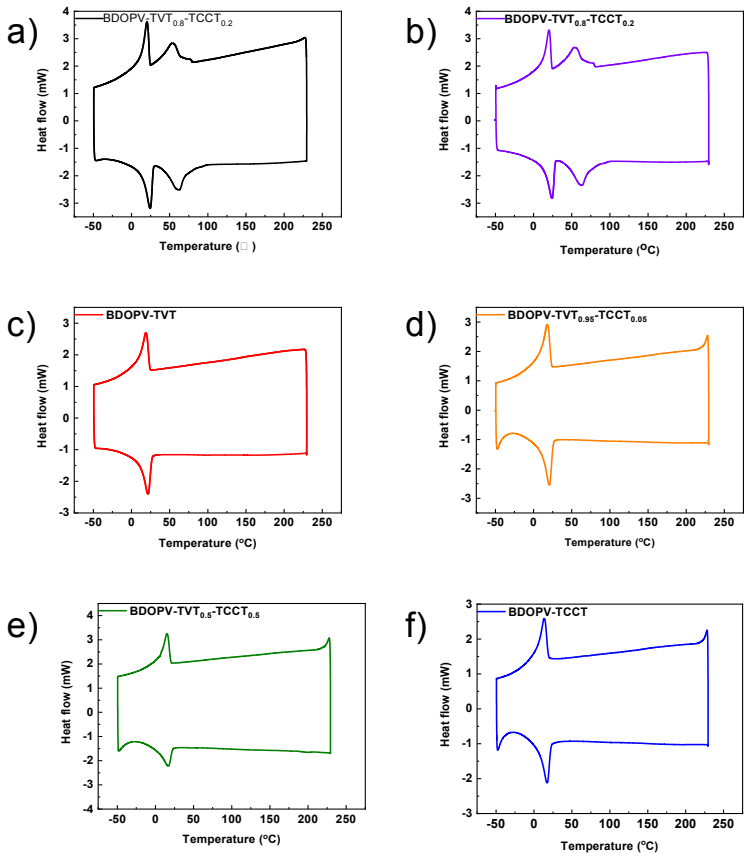

Figure S13. Differential scanning calorimeter traces of re-tested BDOPV-$TVT_{0.8}$-$TCCT_{0.2}$ (a), BDOPV-$TVT_{0.8}$-$TCCT_{0.2}$ (b) BDOPV-TVT (c), BDOPV-$TVT_{0.95}$-$TCCT_{0.05}$ (d), BDOPV-$TVT_{0.5}$-$TCCT_{0.5}$ (e), and BDOPV-TCCT (f).

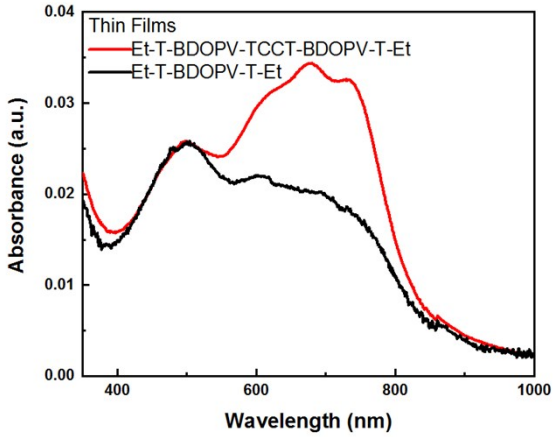

Figure S14. UV-*vis* absorption spectra of small molecules both in intrinsic films. The film absorption of Et-T-BDOPV-TCCT-BDOPV-T-Et did not show obvious red-shift compared with Et-T-BDOPV-T-Et, but only displayed some intensity difference, which may be caused by the folding between fragments of flexible connection. Folding between fragments significantly increased the transition probability between fragments. When the degree of polymerization was further increased, such as BDOPV-TCCT, the corresponding absorbance changed will be more obvious.

5. References

1. Ting Lei, Jin-Hu Dou, Zhi-Jun Ma, Cong-Hui Yao, Chen-Jiang Liu, Jie-Yu Wang, Jian Pei, *J. Am. Chem. Soc.* **2012**, *134*, 20025-20028.
2. Xikang Zhao, Yan Zhao, Qu Ge, Kamal Butrouna, Ying Diao, Kenneth R. Graham, Jian-guo Mei, *Macromolecules* **2016**, *49*, 2601−2608.
3. Ting Lei, Jin-Hu Dou, Xiao-Yu Cao, Jie-Yu Wang, and Jian Pei, *J. Am. Chem. Soc.* **2013**, *135*, 12168–12171.